The Journal of Experimental Biology 206, 181-193

doi:10.1242/jeb.00063

Fine-scale patterns of odor encounter by the antennules of mantis shrimp tracking turbulent plumes in wave-affected and unidirectional flow

Kristina S. Mead[1,*], Megan B. Wiley[2], M. A. R. Koehl[3] and Jeffrey R. Koseff[2]

[1]*Biology Department, Denison University, Granville, OH 43023, USA,* [2]*Environmental Fluid Mechanics Laboratory, Department of Civil and Environmental Engineering, Stanford University, Stanford, CA 93405-4020, USA* and [3]*Department of Integrative Biology, VLSB 3060, University of California, Berkeley, CA 94720-3140, USA*

*Author for correspondence (e-mail: meadk@denison.edu)

Accepted 1 October 2002

Summary

Many marine animals track odor plumes to their source. Although studies of plume-tracking behavior have been performed in unidirectional flow, benthic animals such as crustaceans live in coastal habitats characterized by waves. We compared signal encounters by odor-plume-tracking stomatopods (mantis shrimp) in wave-affected and unidirectional flow in a flume. Stomatopods are small enough that we can study their natural behavior in a flume. They sample odors by flicking their antennules. A thin sheet of laser light illuminating an odor plume labeled with dye [planar laser induced fluorescence (PLIF) technique] permitted us to measure the instantaneous odor concentration encountered by the animal's chemosensory organs (antennules) while it tracked the plume. We simultaneously measured behavior and the high-resolution odor signal at the spatial and temporal scale of the animal. We found that the navigating animal encountered odor filaments more often in wave-affected flow than in unidirectional flow. Odor filaments along the animals' antennules were significantly wider and of higher concentration in waves than in unidirectional flow.

Key words: mantis shrimp, *Hemisquilla ensiguera californica*, stomatopod, chemosensory, plume-tracking, PLIF, wave-affected flow.

Introduction

Many marine crustaceans use water-borne chemical cues in ecologically critical activities such as finding food, mates and suitable habitat, detecting predators and communicating with conspecifics (Caldwell, 1979, 1982; Ache, 1982; Atema and Voigt, 1995; Zimmer-Faust, 1989; Weissburg and Zimmer-Faust, 1993, 1994; Weissburg, 2000). The act of following an odor plume to its source is called 'plume tracking'. In turbulent environments, odor plumes consist of fine filaments containing high concentrations of odor molecules interspersed with the surrounding fluid (Murlis and Jones, 1981; Moore and Atema, 1991; Moore et al., 1994; Weissburg, 2000; Crimaldi and Koseff, 2001; Webster et al., 2001; Crimaldi et al., 2002). Crustaceans sample the fine structure of the odor filaments by moving their antennules through the filaments (Koehl et al., 2001). We are interested in discovering how mantis shrimp (and by extension, other crustaceans) use the information contained in odor filaments to find the source of the odorant.

Initial studies of plume tracking relied on descriptions of plumes as slowly diffusing clouds of chemicals rather than as filamentous, intermittent and dynamic structures. By recording at a point, later investigators showed that odor plumes are intermittent (Zimmer-Faust et al., 1988a,b, 1995; Moore and Atema, 1988, 1991; Atema et al., 1991; Moore et al., 1994; Consi et al., 1995; Dittmer et al., 1995). More recently, planar laser induced fluorescence (PLIF) techniques have shown that odor plumes in water are filamentous (Crimaldi and Koseff, 2001; Webster and Weissburg, 2001; Crimaldi et al., 2002). Koehl et al. (2001) have shown how odor filaments are encountered by a real antennule swept through a realistic plume by computer-driven motor attached to a stationary lobster carapace. Our study examines odor encounter by antennules of a live, odor-plume-tracking stomatopod.

In addition, earlier plume-tracking investigations focused on unidirectional flow. While some species inhabit environments exposed to unidirectional flow (e.g. crabs and crayfish), many others live in coastal habitats and thus experience wave-affected flow. Understanding plume-tracking algorithms requires accurate information about the odor signal encountered by the animal's sensors as it tracks a plume in an environmentally relevant flow field. Our goal in this paper is to answer, for the first time, the following question: what is the instantaneous, fine-scale chemical signal encountered by the mantis shrimp as it tracks an odor plume in wave-affected and in unidirectional flow? This information, correlated with behavior, is the critical first step in deducing the algorithms used by odor-plume-tracking animals.

Mantis shrimp as model systems

We use mantis shrimp (also called stomatopods) as a model

system for examining the ability of crustaceans to track odor plumes. Stomatopods are excellent subjects for chemosensory studies because they depend on chemosensory information for several critical aspects of their life history, including feeding, reproduction, investigating burrows and mediating aggressive interactions with conspecifics (Caldwell, 1979, 1985, 1987; Caldwell et al., 1989). In addition, they occur in many coastal habitats, with and without waves. The external and internal morphology of their chemosensors (located on their antennules) has been measured (Mead et al., 1999; Mead and Weatherby, 2002). We use *Hemisquilla ensiguera californica* because they are active at a cool room temperature, engage in tracking behavior in the flume and are relatively easy to collect and maintain in the laboratory. Their small size (12–20 cm rostrum–telson length) relative to the flume (7.2 m) means that *H. ensiguera* can carry out normal searching and plume-tracking behavior in the flume without being cramped.

Stomatopod chemosensory sampling

Stomatopods (Mead et al., 1999), like many crustaceans (Snow, 1973; Schmitt and Ache, 1979; Reeder and Ache, 1980; Devine and Atema, 1982; Gleeson et al., 1993, 1996; Steullet and Derby, 1997; Hallberg et al., 1997), sample their chemical environment by flicking their second preoral appendages (antennules) through the surrounding fluid. In stomatopods (and some lobsters), the asymmetry of the flick ensures that already-sampled fluid is cleared out, so that new odor-containing fluid can come into contact with the animal's chemosensors (Mead and Koehl, 2000; Goldman and Koehl, 2001; Koehl et al., 2001). The stomatopod chemosensory sensilla (termed aesthetascs) are long, slender cuticular structures located in rows of three on the distal dorsal surface of a filament that arises from the lateral antennule filament (Mead et al., 1999; Mead and Koehl, 2000). Thus, the aesthetasc-bearing filament of stomatopods is homologous to the aesthetasc-bearing lateral filament of decapod crustaceans. The aesthetascs are heavily innervated with bipolar sensory neurons [14–20 per aesthetasc in *Gonodactylaceus mutatus*, another stomatopod species (Mead and Weatherby, 2002)]. Depending on the size of the animal, the region of the antennule covered with aesthetascs ranges from approximately 3 mm to 10 mm long (K. S. Mead, unpublished data).

Flicking also facilitates odor molecule arrival at the sensors (Stacey et al., 2002). When a mantis shrimp flicks its antennules, the boundary layer surrounding the aesthetascs thins, so that odor molecules need only diffuse a short distance before encountering the aesthetasc surface (Mead and Koehl, 2000; for other taxa, see also Louden et al., 1994; Koehl, 1995; Koehl et al., 2001). In addition, more odor-containing fluid moves through the array of aesthetascs during the flick outstroke than at other times. As molecule capture is greatest and fastest during the flick outstroke (Stacey et al., 2002), we confined our analysis to the signal encountered by the aesthetasc-bearing portion of the antennule during flicks only. When tracking odors, mantis shrimp increase their flicking rate to 2–4 Hz as long as they are within the plume.

Plume structure

Several parameters affect the structure of an odor plume and, thus, how the plume is encountered by navigating animals. When the source is low momentum and flush with the bottom, the plume is shaped and transported exclusively by the ambient flow (Fischer et al., 1979). Characteristics of the plume's odor filaments in time and space therefore depend on such flow conditions as the mean velocity, the turbulence level and the gradient of flow speed above the substratum (the current boundary layer).

The presence of surface waves changes the free stream velocity so that it varies in time. The superposition of waves over the current also affects the bottom shear stress and, therefore, the shear velocity (u_*), which is a surrogate for the shear stress at the bottom boundary and an indicator of turbulence levels in the water column. For a wave-affected flow, the time-averaged shear stress increases over a rough boundary (Grant and Madsen, 1979), but the effect of the waves on flows over a smooth bottom is more complex (Kemp and Simons, 1982). Specifically, Kemp and Simons (1982) did not observe an increase in time-averaged shear stress over a smooth bottom, but rather periodic increases in u_*, which exceeded the time-averaged mean by a factor of two at times. Furthermore, they found that maximum turbulence levels in the water column occurred after the peaks in shear velocity. The impact of this periodic behavior on the dispersal of odor plumes has not yet been fully established. We chose to study a flow with a smooth bottom initially for two reasons: first, we believed it was important to start with the physically simpler case; second, we needed to provide the digital camera with optical access from below the tank. Crimaldi and Moore are currently studying a similar problem with rough boundaries (J. P. Crimaldi and P. A. Moore; personal communication).

To date, all plume-tracking behavioral experiments have been performed in unidirectional flow or in stationary flow with jets (Devine and Atema, 1982; Atema, 1985, 1988; Moore and Atema, 1991; Moore et al., 1991, 2000; Weissburg and Zimmer-Faust, 1993, 1994; Consi et al., 1995; Finelli et al., 2000). While crustaceans living in estuaries or streams do experience unidirectional flow, the water motion at many coastal sites is affected by waves. Therefore, the flow encountered by most coastal benthic organisms is wave-affected, with flow speed and direction changing on the time scale of seconds (e.g. Koehl, 1977, 1982, 1984, 1996). Odor plumes in these environments may behave differently to odor plumes in unidirectional flow. The present study examines how stomatopod chemosensors encounter odor filaments as the animals track plumes in both wave-affected and unidirectional flow.

Imaging odor plumes

Previous work on odor plumes dispersing in benthic boundary layers has involved making single point measurements of fluctuating concentrations downstream from the source (Zimmer-Faust et al., 1988a,b, 1995; Moore and Atema, 1988, 1991; Atema et al., 1991; Moore et al., 1994;

Consi et al., 1995; Dittmer et al., 1995; Consi et al., 1995). Point measurements cannot record the instantaneous spatial structure of the plume or the temporal evolution of specific features. Both of these factors are likely to be important in chemotaxis. By contrast, a new method for visualizing flow, PLIF, uses a light sheet and dye that emits light when it is stimulated by a laser to generate a large two-dimensional slice of the flow. PLIF allows for the collection of concentration information seen by the entire array of sensors along the animal's antennules. This makes it possible to follow the evolution of specific plume structures over time and to monitor the plume dynamics near the animal. For example, PLIF images reveal if times of zero concentration at the sensor reflect parcels of clean fluid within the odor plume or a meandering of the plume to the side of the sampling volume. In this study, we take advantage of the high spatial and temporal resolution available with PLIF to determine the instantaneous chemical signal encountered by mantis shrimp as they track the odor plume to its source.

Odor signal characterization

As there is almost no published chemosensory neurophysiology on mantis shrimp, we do not know which signal characteristics are important to stomatopods. By analogy to lobsters, it seems likely that stomatopods detect peak odor concentration and odor pulse duration (Gomez and Atema, 1996a,b; Gomez et al., 1999). We use filament width as a spatial analogy of pulse duration. In addition, models and experiments suggest that sensory cells can distinguish between different rates of increasing odor concentration (onset slope; Moore, 1994; Kaissling, 1998a,b; Zettler and Atema, 1999; Rospars et al., 2000). We therefore characterize the odor filaments encountered by stomatopod antennules during flicking in terms of their maximum and mean concentration, their width and their spatial sharpness, a parameter that we introduce as a spatial surrogate for onset slope.

We will characterize *H. ensiguera californica* odor sampling in wave-affected and unidirectional flow focusing on the following elements: maximum and average odor concentration along the antennule, filament width along the antennule and filament sharpness.

Materials and methods

Field flow measurements

Hemisquilla ensiguera californica (Owen 1832) lurk at the mouths of their burrows sampling passing odors with their antennules 0.01–0.03 m above the substratum. To estimate water velocities near the animal's antennules, water velocities near 11 *H. ensiguera californica* burrows were measured by videotaping (Sony CCD-TR-700, Quest Pro-shot housing; 30 frames s^{-1}) particles suspended in the water moving past measuring tapes on the substratum in line with the onshore–offshore axis and perpendicular to that axis. Each frame was split into two fields, effectively raising the framing rate to 60 frames s^{-1}. The burrows were located in gently to moderately sloping sandy mud substrata at 10–20 m depth in Willow Cove, off the island of Santa Catalina, CA, USA. The videotapes were digitized using NIH image software. Water velocities were measured for 1–10 min per burrow.

Stomatopod collection and handling

H. ensiguera californica were collected from Willow Cove by SCUBA divers. Animals were maintained in large containers of artificial seawater ('Instant ocean') at 17°C, were fed mussels and crabs twice per week, and were subjected to a 16 h:8 h light:dark cycle. Prior to experiments at the Stanford Recirculating Wave-Current Flume (RWCF), the animals were acclimated to 20°C.

Pilot experiments to determine odor source, concentration, dye mixture and effect of laser

Attractive odor substances and concentrations were determined through extensive Y-maze experiments. The Y-maze consisted of a deep U-shaped channel (60 cm long × 13 cm deep × 10 cm wide) leading to a fork where two additional channels (same dimensions) branched off at 30°. Seawater was gravity fed into the tips of the two branches where it flowed through collimators made of banks of straws, resulting in a 1 cm s^{-1} laminar flow through the arms of the maze. The animal was placed in the base of the maze, just upstream of the flow outlet. During experiments, an odor and/or dye mixture was added to the incoming water in one of the two arms (chosen randomly) without altering the flow rate. All experiments were done in the dark, with no visual, acoustic or hydrodynamic stimulation. The experimenter was hidden behind a screen. Trials were videotaped using a digital low-light-sensitive camera (Sony DCR-TRV9). At the start of the experiment, a partition blocking the animal's access to the maze was removed and the mantis shrimp was allowed to navigate upstream. A successful find required that the animal navigated up the correct branch to the collimators. 75 trials were performed on 11 *H. ensiguera californica* ranging in size from 93 mm to 123 mm rostrum–telson length using mussel and squid extracts as attractive odors. The extracts were prepared by homogenizing fresh mussels or squid in seawater and filtering out solid material. Protein concentrations were determined by the Bio-Rad Standard Protein Assay (Bio-Rad 500-0112). The Y-maze trials tested the 'attractiveness' of squid and mussel protein concentrations from 4×10^{-6} mg ml^{-1} to 10^{-3} mg ml^{-1}, with and without rhodamine or fluorescein dyes (10^{-10}–10^{-4} mol l^{-1}).

In other preliminary tests, the stomatopods were exposed to the laser light sheet used in the flume.

The experimental facility

The plume-tracking experiments were conducted in the RWCF located in the Environmental Fluid Mechanics Laboratory at Stanford University (Fig. 1). The flume is 1.22 m wide and 12.50 m long, with a test section length of 7.32 m. The depth of water was 0.41 m for the unidirectional flow

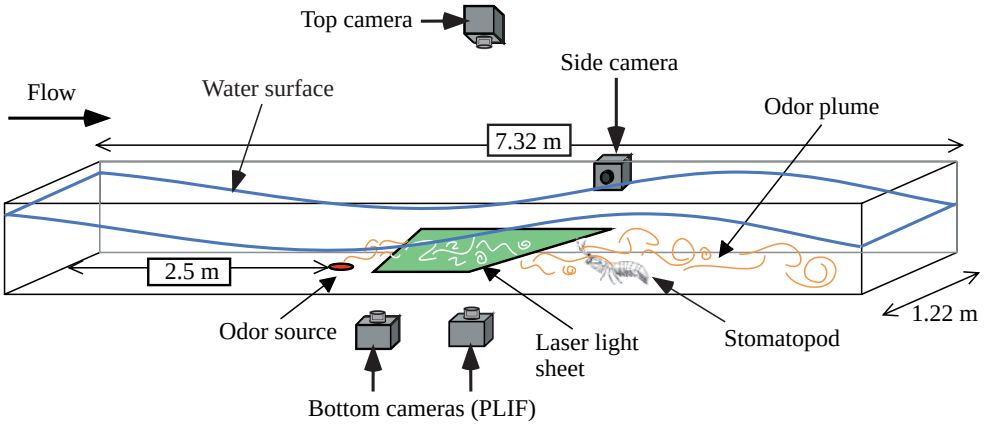

Fig. 1. Flume set-up. The experimental set-up consisted of the Recirculating Wave-Current Flume (RWCF) set to produce either 5 cm s^{-1} unidirectional flow or 0.5 Hz waves with a velocity range of –5 cm s^{-1} to 9 cm s^{-1} at a height of 2 cm, the height of the stomatopod antennules. A laser light sheet fluoresced the rhodamine-spiked odor plume, so that the structure of the odor plume could be recorded by the two planar laser induced fluorescence (PLIF) cameras filming through the bottom of the flume and the top camera filming through the water's surface.

condition and 0.383±0.012 m for the wavy condition. A variable-frequency drive (VFD; Mitsubishi FR-E520-7.5K-NA) controlling a pump [Johnston Pumps 10 PO 1 stage propeller driven by US Electrical Motor H11902, 10 Hp (7.4 kW)] allowed us to set the mean velocity. Vortical structures produced by the pump were broken up in the expansion section and upstream using a series of grids and PVC pipes. The wave maker, located at the upstream wall of the flume, consisted of a flexible 9.5 mm thick polycarbonate plate fixed 53.9 cm below the mean water level for the unidirectional or wave-affected flows, respectively. A servomotor and linear actuator attached at the top of the plate moved the paddle back and forth according to a 0–10 V analog input signal, generating surface waves. Additional information about the flume is reported in Pidgeon (1999).

Flow conditions

The VFD and wave maker were able to produce hydrodynamic conditions near the tank floor similar to those found in the *H. ensiguera californica* habitat off the coast of Southern California. Specifically, we used 0.5 Hz waves with a velocity range of –0.05 m s^{-1} (upstream) to +0.09 m s^{-1} (downstream) at a distance of 0.02 m (an average antennule height) above the flume bottom. We also ran experiments without waves, using a unidirectional flow speed of 0.05 m s^{-1}. This water velocity is experienced by some stomatopod species living in sheltered habitats, and is also similar to that used in some previous studies of plume tracking in other crustaceans (e.g. Weissburg and Zimmer-Faust, 1993).

The source

The plume was created by 'oozing' a neutrally buoyant mixture of fresh mussel extract (0.3–0.75 mg ml^{-1} protein) marked with 10 p.p.m. rhodamine 6G dye through a sponge (0.025 m thick, 0.01 m diameter) flush with the floor of the tank. This low-momentum source was designed to mimic a diffusing odor source on the ocean floor, such as a dead, partially buried fish or an open stomatopod burrow (Crimaldi and Koseff, 2001). The dimensionless Schmidt number, which is the ratio of the kinematic viscosity of water (m^2 s^{-1}) to the coefficient of molecular diffusion of the dissolved element in water (m^2 s^{-1}), is 1250 for the dye and 1000 for the amino acids in the mussel extract. The similar Schmidt numbers ensure that when we image the dye filaments, we are imaging the actual odor filaments as well.

Planar laser induced fluorescence (PLIF)

To generate images of the thin slice of the odor plume at the height of the mantis shrimp's antennules, we illuminated the dyed plume with a thin sheet of laser light and recorded images of the fluoresced light (PLIF). The luminescence intensity recorded by the camera is directly proportional to the concentration of the dye, and thus to the odorant concentration. The apparatus used to collect the PLIF data, illustrated in Fig. 1, was based on the experimental set-up of Crimaldi and Koseff (2001). The light sheet (2.5 mm thick) was created by sweeping the beam of a laser (Coherent Innova 90 Argon Ion; Coherent, Inc., Santa Clara, CA, USA; 0.84 W, 514.5 nm wavelength) in a plane parallel to and 2 cm above the flume floor using a moving magnet optical scanning mirror (Cambridge Technology model 6800 HP; New Methods Laser, Largo, FL, USA) controlled by a LabView-generated analog signal. The sweeping of the beam acted as a shutter system for the CCD cameras (Silicon Mountain Design model SMD-1M15 and 1M30; Uniforce Sales and Engineering, Milpitas, CA, USA; 1024 pixels×1024 pixels) positioned below the tank. When the dye/odor mixture in the water was illuminated by the laser, the CCD chip recorded the fluorescence as a 12-bit gray scale intensity. A narrow-bandpass optical filter (center wavelength of 557 nm, bandwidth of 45 nm) restricted the luminescence available to the chip to the emission wavelengths of the rhodamine (555 nm, 40 nm bandwidth).

Flume experimental protocol and data collection

Each animal tested in the flume (six animals, 144 trials, 90 of which resulted in plume-searching and/or plume-tracking behavior) was unfed during the 48 h prior to an experiment and was placed in the flume the night before the experiment. Each animal was exposed to the tested flow regime (unidirectional flow or wave-affected flow) in the dark for one hour before the experiment. Each animal was only used once per day of

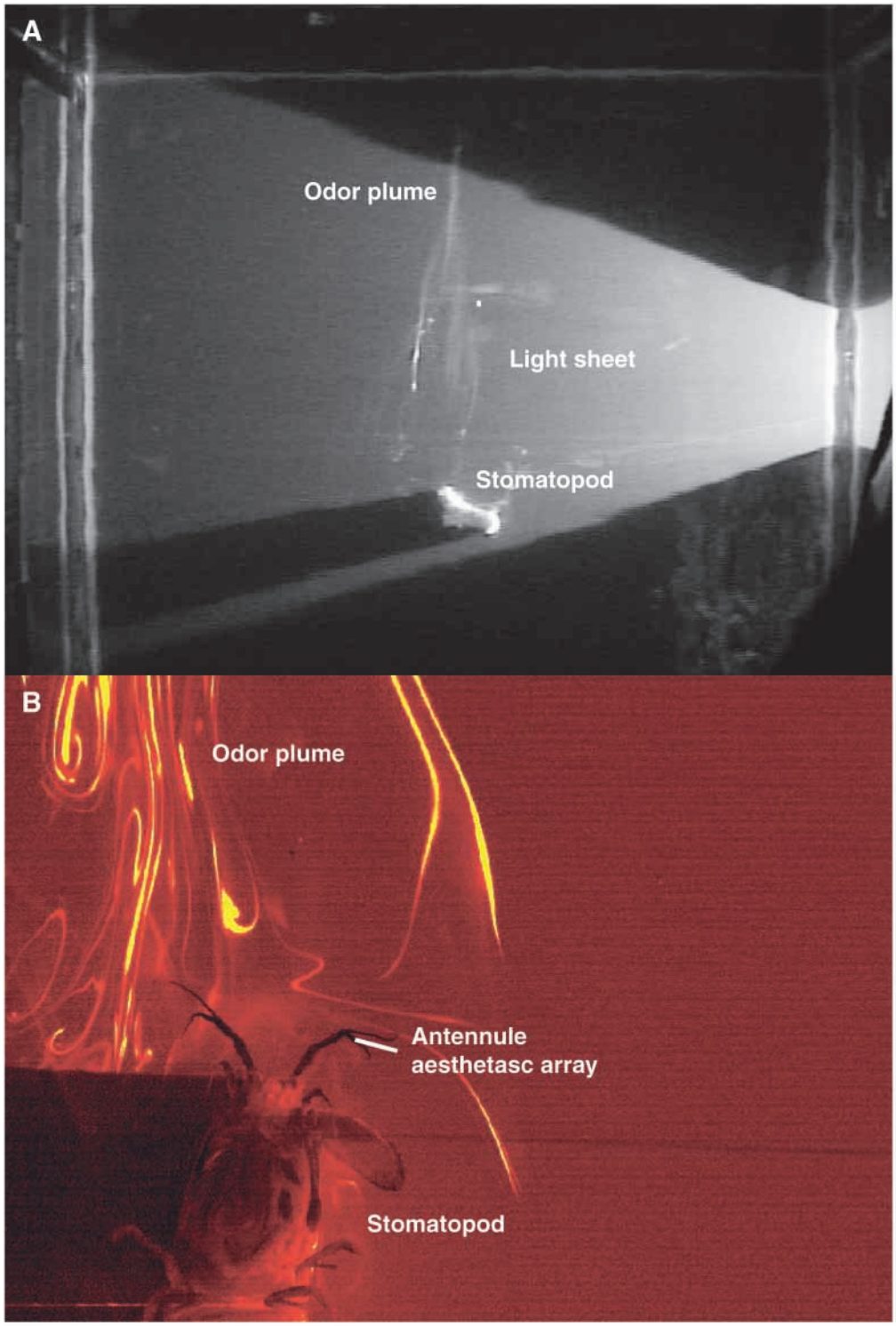

Fig. 2. Stomatopod in flume. (A) An image of *Hemisquilla ensiguera californica* navigating an odor plume recorded by the overhead camera. (B) *H. ensiguera californica* plume tracking within the field of view of the downstream planar laser induced fluorescence (PLIF) camera recording from below. Both images are from successful searches in wave-affected flow.

experimentation to minimize learning and other effects of previous exposure.

Once the source was turned on, the animal was released away from the plume approximately 2.4 m downstream. We recorded searching behavior with a stationary overhead video camera (Sony DCR-TRV9; 0.80 m×0.80 m field of view). When possible, a second video camera (Sony CCD-TR101) was used to record antennule position from the side of the tank. If the animal passed over one of the PLIF cameras (centered at 0.47 m and 0.76 m downstream of the source), we collected 10 s of images at 15 Hz. This time period, limited by computer RAM, was generally adequate to record the animal passing through the entire field of view (0.18×0.18 m). As stomatopods carry the aesthetasc-bearing portion of their antennules (5–10 mm long, depending on the size of the animals tested) 1–3 cm above the substratum, and as stomatopods flick mostly in a horizontal plane while plume tracking, almost all of the observed flicks were in the plane of the light sheet. Out of the nearly 200 flicks recorded by the PLIF camera, only two or three were out of the light sheet (and were thus out of focus). We continued recording with the overhead camera until the animal encountered the source or aborted the search.

Fig. 2A and Fig. 2B show examples of images taken with the overhead camera and a PLIF camera, respectively. The PLIF camera chips pixel arrays provide spatial resolution of 180 μm in the plane of the sheet. This is smaller than the smallest length scale for turbulent structures (630 μm; the Kolmogorov microscale) at the height of the animals' antennules but is larger than the theoretical smallest scales for the plume filaments (the Batchelor scale, 20 μm).

Image correction and calibration

Background images taken without the presence of the plume and animal were used to correct for the background fluorescence and dark response of the camera, variations in light sheet intensity from attenuation by background dye and other cross-stream non-uniformities, as well as differential pixel responses to luminescence by the CCD chip (Crimaldi and Koseff, 2001). We minimized photobleaching by chosing rhodamine 6G as the fluorescing dye, because it exhibits as much as 62-fold less photobleaching than fluorescein (Crimaldi, 1997), and by using a low source concentration of dye. Approximately 0.001% of the pixels in the camera chip do not function properly. These pixels were assigned a concentration value interpolated from their adjacent pixels. To reduce shadowing and scattering of laser light by moving particles, we kept the water well-filtered and the tank covered. Flat field Micro-Nikkor camera lenses were selected to reduce curvature effects around the edges of the images. The laser beam sweep was restricted to 20 ms to reduce image distortion caused by the moving fluid. Further details of image correction are described in Crimaldi and Koseff (2001).

Luminescence intensity recorded as a 12-bit value by the PLIF cameras was converted to rhodamine concentration by imaging jets of known concentration. We were able to distinguish concentrations as low as 0.1% of the source concentration (equivalent to an odor concentration of 0.3–0.75 μg protein ml^{-1} fluid) from non-odored background fluid. Our concentration resolution was 0.01% and 0.04% of the source for the wave-affected and unidirectional tracks, respectively.

Image interrogation

To quantify signal characteristics at the animals' antennules, we determined the location of the base and tip of the aesthetasc-bearing filament in all of the frames in which the animal was flicking. Recall that physical and mathematical models suggest that mantis shrimp sample fluid only during antennular flicking (Mead and Koehl, 2000; Stacey et al., 2002; see also Koehl et al., 2001 for lobster antennules encountering odor filaments during flicking). We chose pixel locations along the instantaneous upstream portion of the antennule. For the wave-affected flow, we chose pixels on the side of the aesthetasc-bearing filament that was encountering flow (either upstream or downstream, depending on the motion of the water and of the antennule). We determined these locations and made subsequent calculations with user-written programs in Igor (WaveMetrics, Inc., 4.0, Lake Oswego, OR, USA).

In our discussion of signal characteristics, we distinguish between physical characteristics of the plume *per se* and characteristics of the sampled plume, which are functions not only of the plume but also of the size, shape and flicking motions of the antennules and the location of the animal. We use the phrase 'plume characteristics' to refer to the plume itself, and the words 'sampled plume' to refer to characteristics of the signal at the animal's antennules.

Calculations

We determined the number of flicks per track and the time that the antennules were in the field of view of the PLIF cameras by counting frames from the below-flume camera. The instantaneous velocity was calculated as the change in position of an animal between successive frames divided by the framing rate (30 frames s^{-1}). We averaged the instantaneous velocity of an animal over all frames of the plume-tracking event to generate an average speed. We calculated the net-to-gross path length ratio (a measure of the straightness of the animal's locomotory path) by dividing the distance traveled in the direction of the source from the starting position by the total distance traveled. Average speed and net-to-gross path length ratio were calculated from the longer movies taken with the overhead camera using only the segments that corresponded to the short PLIF movies obtained from the camera below the flume.

Once we determined the concentration along the animal's antennules during flicks in the PLIF movies, we calculated a number of different signal characteristics, which are described below. Unless noted, all of our concentration measurements were normalized by the source concentration. We automated our calculations with programs in Igor.

Available signal

The available signal is a measure of the amount of dye 'near' the animal (within the field of view of the camera). We used the available dye signal as a way to (1) monitor the physical variability of the plume, (2) compare plume structure in wave-affected and unidirectional flow and (3) normalize the amount of dye and odor protein available near the animal during tracking events. These calculations enabled us to compare tracking events with lots of odor and dye near the animal (high available signal) with tracking events when there was less odor and dye near the animal due to plume meander or imperfect alignment with the light sheet (low available signal). We calculated both mean and maximum available signal. We determined the mean available signal by averaging the pixel intensity of all the pixels not covered by the animal or in the animal's shadow in each frame of the below-flume (high-resolution) movies. The mean available signal per frame was then averaged over all frames of the track. The maximum available signal was calculated by recording the maximum pixel intensity per frame and then averaging the maximum pixel intensity over all frames. Both the mean and the maximum available signal were used to compare plume structure in unidirectional and wave-affected flow (Fig. 5), but only the mean available signal was used to normalize the filament concentration (Fig. 7). Unlike our other measurements, the available signal takes into account all of the signal near the animal (see Fig. 2B). By contrast, our other parameters (such as maximum and average concentration, filament width and filament sharpness) measure some aspect of the signal as it is encountered by the edge of the aesthetasc-bearing portion of the mantis shrimp's antennule (Fig. 3).

Percentage of flicks encountering signal above background

As stomatopods appear to sample odors only during flicking, we determined the percentage of flicks that encountered some signal along the antennule at concentrations above background (the lowest level of rhodamine detectable by the camera) for each track to see if there was a difference in the frequency with which signal was detected between unidirectional and wave-affected flow. Any amount of signal over background was considered to be an encounter.

Filament concentration

To further quantify the concentration signals encountered by the antennules, we determined: (1) the concentration of the brightest pixel along the antennule (maximum concentration) and (2) the mean of the concentrations of all the pixels along the antennule (mean concentration). These maximum and mean concentrations were measured for each frame during a flick outstroke and were normalized by the source concentration. These values were averaged over all the flicks in an entire movie, so that each tracking event gave rise to one (mean) maximum concentration and one (mean) mean concentration (Fig. 6). We also normalized the concentration data by the available signal to account for the differences in the plume among experiments (Fig. 7). Filaments that were thinner than the pixel width appeared to have an artificially low concentration value, as the camera integrates intensity over a pixel.

Filament width

We defined the width of an encountered odor filament as the spatial distance along an antennule over which the concentration remained above the background value of the interspersed water. There were often multiple odor filaments along the antennule in a single flick. Filament widths were averaged over an entire movie (N=26–69 per movie). Filaments that were thinner than the pixel width appeared to be artificially wide, as the camera integrates intensity over the pixel. Filaments could also have been recorded as artificially wide depending on how they intersected the 2.5 mm thick light sheet.

Filament sharpness

Filament sharpness was defined as the ratio of the maximum concentration (normalized by the source strength) to the spatial distance from the edge of the filament to the point of maximum concentration (normalized by the source diameter). This parameter, which quantifies the increase in concentration as a function of space, bears a close relationship to filament onset slope, which is the increase in concentration as a function of time. Previous studies suggest that onset slope may be an important navigational cue (Moore and Atema, 1991; Moore, 1994; Atema, 1995; Gomez and Atema, 1996a,b; Kaissling, 1998a,b; Rospars et al., 2000). The measurement techniques used in these earlier studies did not make it possible to examine fine spatial features along the antennule. PLIF enables us to quantify filament sharpness for the first time. In analogy to the importance of contrast in vision (Schmidt-Nielsen, 1990), filament sharpness may be important in plume tracking.

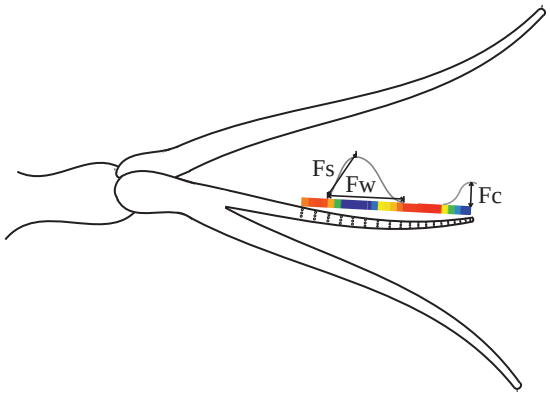

Fig. 3. Signal characteristics. Fc, filament concentration: the maximum concentration per filament. Fs, filament sharpness: the maximum concentration of a filament divided by the distance from the edge of the filament to the point of maximum concentration. Fw, filament width: the distance along the antennule over which the concentration is above background.

Statistics

Standard deviations (S.D.) were calculated within Excel (Microsoft, 1997). Model II analyses of variance (ANOVAs) were calculated using Statview (v. 5.0, SAS Institute Inc., Cary, NJ, USA).

Results

Field flow measurements

At the height of the antennules (approximately 1–3 cm above the substratum), the flow along the substratum under the waves was roughly oscillatory, with peak velocities of approximately 0.07 m s^{-1} (K. S. Mead and M. O'Donnell, unpublished data).

Preliminary investigations (Y-maze studies)

The most successful attractant was 10^{-4} mg ml^{-1} mussel extract, which elicited a response during 76±31% of the trials, with the mantis shrimp being able to correctly find the source of the attractant in 78±19% of the trials that elicited a response (mean ± S.D.; N=6 animals, 3–20 trials per animal). Further Y-maze experiments showed that the presence of rhodamine did not stimulate the stomatopods to begin searching and did not impair the ability of the stomatopods to find the attractive compound in the mussel extracts. In addition, the Y-maze experiments showed that the ability to find the odorant did not improve with experience. Our other tests showed that exposure to the laser light sheet did not affect the stomatopod's behavior in any visible way.

Plume-tracking behavior in the flume

Mantis shrimp exhibited plume-searching/tracking behavior in 90 out of the 144 times that they were placed in the flume.

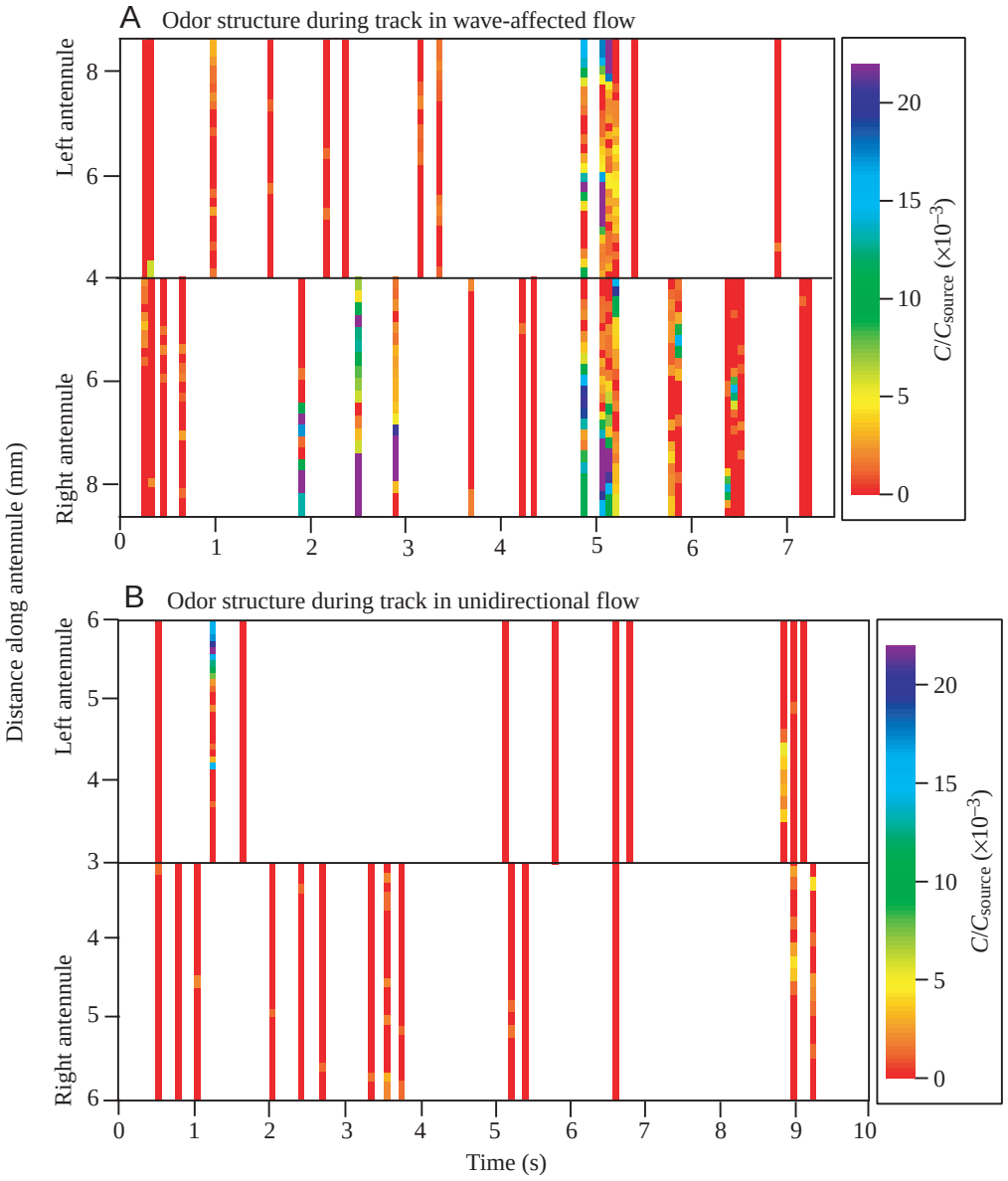

Fig. 4. Fine-scale odor structure along the antennule during flicking (C), normalized by source concentration (C_{source}). (A) Odor concentration along the antennules as a function of time in wave-affected flow. (B) Similar information from a successful track in unidirectional flow. These panels show the odor concentration along each antennule during flicking, which is when the animal samples odors. Each vertical bar indicates a flick. In most cases, a flick lasts one frame only, but in six cases, the flick takes two frames to complete. The top portion of each panel shows odor concentration along the left antennule, and the bottom portion shows odor concentration along the right antennule during the same successful track. Only odor structure encountered by the outer portion of the antennule (where the aesthetascs are located) is shown. The odor concentration is color-coded; red indicates background levels, yellow indicates low concentration, and blue indicates high concentration.

Out of these 90 trials by six animals, only seven plume-tracking events [four in wave-affected flow (all from two individuals) and three in unidirectional flow (all from one individual)] had portions that extended into the field of view of the PLIF camera, contained odor/dye filaments in the same frames within the field of view of the PLIF camera, showed flicks within the laser light sheet during the 10 s that we were able to store per tracking event, and were in sufficient focus to analyze quantitatively. Only one portion of the track was analyzed per plume-tracking event. All of the track segments presented in this manuscript were within the field of view (0.18 m×0.18 m) of the camera centered 0.76 m downstream of the source. While the sample size of tracks analyzed with PLIF is small, we believe that these seven tracks are representative of a much larger number of plume-tracking events recorded by the overhead camera.

Common features of plume-tracking events

In all seven plume-tracking events analyzed with PLIF, the mantis shrimp tracked the odor plume to its source. The duration of the entire tracking event, length of time that the animal's head and at least one antennule were visible, number of flicks per track, number of flicks per second, mean animal speed, and net-to-gross path length (a measure of path curviness) were indistinguishable between the tracks in wave-affected flow and the tracks in unidirectional flow (Table 1).

Fine-scale odor structure

Fig. 4 shows the fine-scale odor structure along the antennules during a plume-tracking event in wave-affected flow (Fig. 4A) and in unidirectional flow (Fig. 4B). Each vertical bar shows the odor concentration as a function of

Table 1. *Summary information about plume-tracking events in wave-affected and unidirectional flow*

	Tracks in wave-affected flow (N=4)	Tracks in unidirectional flow (N=3)	ANOVA P values
Number of flicks	27.0±6.6	27.7±8.1	0.91
Flicks per second	3.3±0.5	3.2±0.7	0.85
Time at least one antennule in close-up field of view	8.1±1.0 s	8.8±2.2 s	0.62
Time of entire track (overhead camera)	34.3±14.5 s	48.8±24.0 s	0.41
Reached source (overhead camera)	100%	100%	N/A
Average speed (overhead camera)	1.4±0.54 cm s^{-1}	0.90±0.36 cm s^{-1}	0.22
Net-to-gross path length ratio (overhead camera)	0.25±0.19	0.31±0.06	0.65

distance along the antennule during a flick. When stimulated, *H. ensiguera californica* sample at approximately 2–4 flicks s^{-1} but can flick in short bursts of up to 10 flicks s^{-1}. Note that the antennules operate independently. The odor signal can be quite sparse, so that many flicks fail to intercept a filament. Even when a filament is encountered, it only covers a small portion of the aesthetasc-bearing portion of the antennule, especially in unidirectional flow. Nonetheless, all the plume-tracking events analyzed here resulted in the stomatopod successfully finding the source of the odorant.

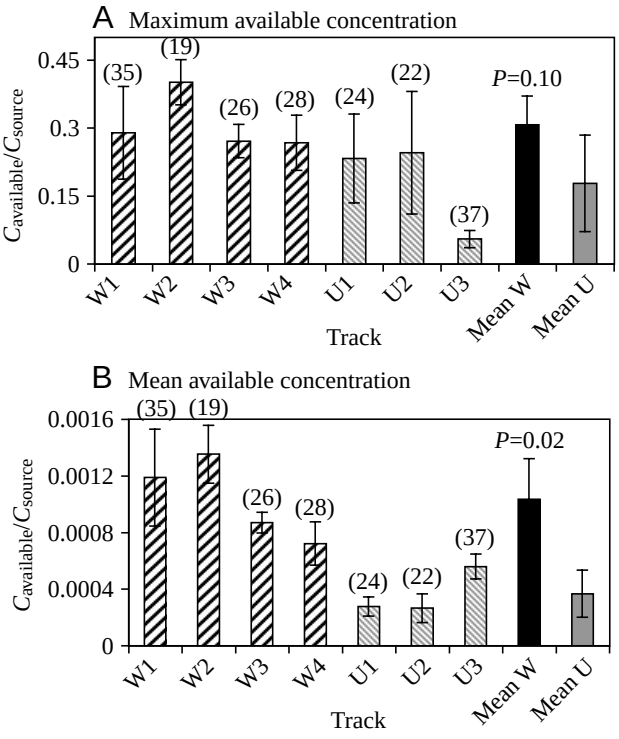

Fig. 5. Available source concentration ($C_{available}/C_{source}$). (A) The maximum available source concentration as a function of the track. (B) The mean available source concentration. Tracks in wave-affected flow are shown in bars with black diagonal stripes (mean of all four wave-affected flow tracks in black bar), and tracks in unidirectional flow are shown in bars with gray diagonal stripes (mean of all three unidirectional flow tracks in gray bar). Values are means ± S.D. The number of flicks (N) for each track is shown in parentheses above the bar.

Available signal

Fig. 5A shows the maximum available signal concentration

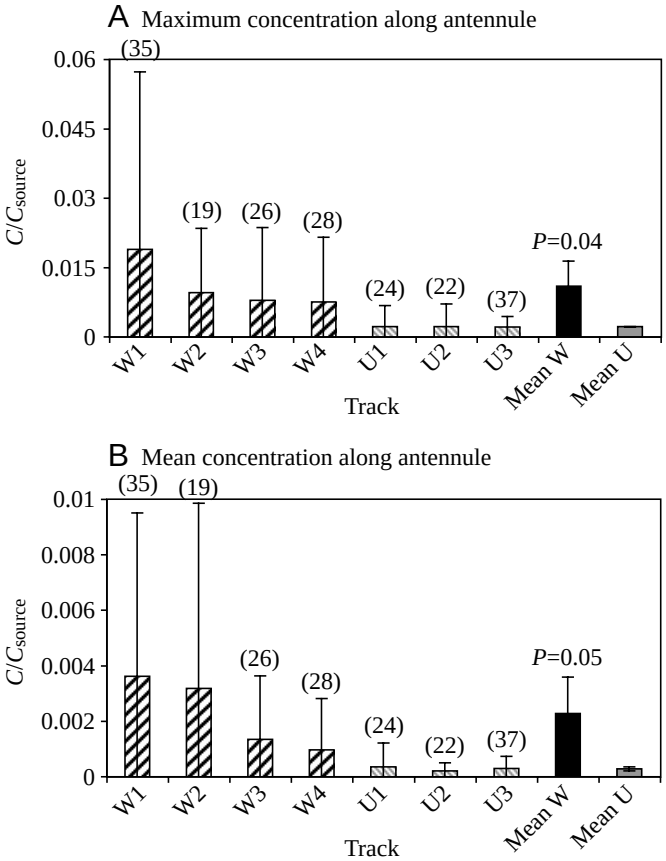

Fig. 6. Odor concentration along the antennule (C) normalized by source concentration (C_{source}). (A) The maximum concentration along the antennule as a function of the track. (B) The mean concentration along the antennule. Tracks in wave-affected flow are shown in bars with black diagonal stripes (mean of all four wave-affected flow tracks in black bar), and tracks in unidirectional flow are shown in bars with gray diagonal stripes (mean of all three unidirectional flow tracks in gray bar). Values are means ± S.D. The number of flicks (N) for each track is shown in parentheses above the bar.

(a measure of the amount of dye 'near' the animal; i.e. in the field of view of the high-resolution camera) in all the tracks, and Fig. 5B shows the mean available signal concentration in all the tracks. Both graphs demonstrate the variability of the plume over time. In general, the maximum available concentration is similar in unidirectional and wave-affected flow. By contrast, the mean concentration available to animals tracking plumes in wave-affected flow is greater than that available to mantis shrimp tracking plumes in unidirectional flow.

Flicks encountering signal

When stomatopods track a plume in wave-affected flow, a greater percentage of the flicks (85±7%; N=4 plume-tracking events) encounters some signal than when the stomatopods track a plume in unidirectional flow (63±9%; N=3 plume-tracking events, P=0.01). Furthermore, stomatopods in wave-affected flow encounter more filaments than stomatopods in unidirectional flow (39.3±6.4 *versus* 21±6.9, P=0.02).

Odor concentration along the antennules

When the odor concentration is normalized by dividing by the source concentration, both the maximum and the mean odor concentration along the antennule are greater in wave-affected flow than in unidirectional flow (Fig. 6). However, when the odor concentration is normalized by the available concentration, the maximum and mean concentrations along the antennule in unidirectional and wave-affected flow are indistinguishable (Fig. 7).

Filament width along the antennule

Odor filaments encountered by the antennule appear to be wider, on average, in wave-affected flow than in unidirectional flow (Fig. 8). However, the greater variance of filament width in wave-affected flow indicates that there is a greater range of widths in the filaments in wave-affected flow.

Filament sharpness

The filament sharpness (a measure of the increase in concentration as a function of space) in wave-affected and unidirectional flow was not statistically different (Fig. 9). If we assume that the turbulence is isotropic (shows no directional preference) at the level of the antennules, and that filaments do not evolve significantly over short time scales, then this suggests that onset slopes do not differ significantly in wave-affected and unidirectional flow. There may, however, be some difference that we cannot detect with our spatial resolution.

Discussion

Our experiments show what an odor plume looks like on the scale of the antennule. This is only the second time that such a data set on the level of an antennule has been created (Koehl et al., 2001). It is the first time it has been possible to collect such data for a living animal engaged in tracking, and the first time such data have been collected for a plume in waves.

Characteristics of odor plumes in unidirectional and wave-affected flow

Previous models of odor plumes (e.g. Bossert and Wilson, 1963) assumed a cloudlike, gradually dissipating Gaussian structure. Our experiments confirmed that odor plumes are actually sparse and extremely intermittent in time and space (Crimaldi and Koseff, 2001). Odor plumes in both unidirectional and wave-affected flow consist of very thin filaments of high concentration interspersed with clean water. The maximum available concentration is similar in both flow conditions, but the mean available concentration is greater in wave-affected flow than in unidirectional flow. This suggests that filaments in wave-affected flow are wider on average than

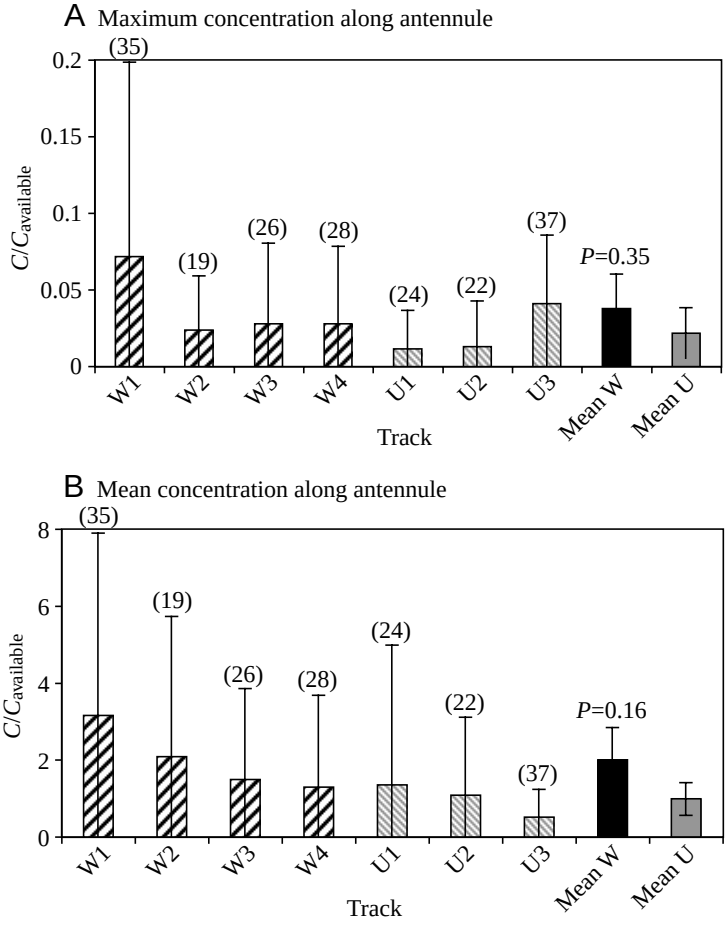

Fig. 7. Odor concentration along the antennule (C) normalized by available signal concentration ($C_{available}$). (A) The maximum concentration along the antennule as a function of the track. (B) The mean concentration along the antennule. Tracks in wave-affected flow are shown in bars with black diagonal stripes (mean of all five wave-affected flow tracks in black bar), and tracks in unidirectional flow are shown in bars with gray diagonal stripes (mean of all three unidirectional flow tracks in gray bar). Values are means ± S.D. The number of flicks (N) for each track is shown in parentheses above the bar.

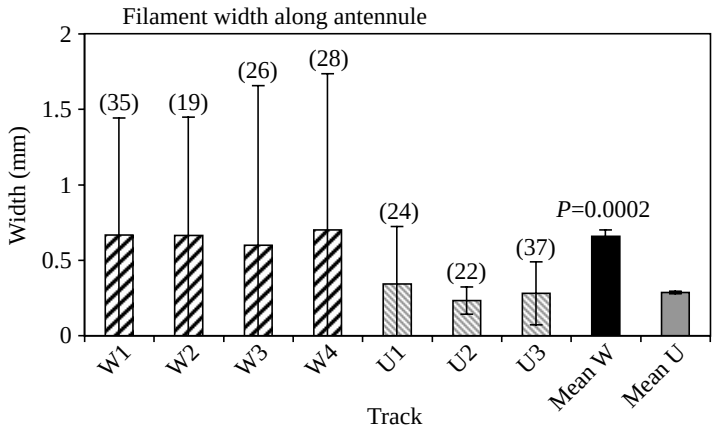

Fig. 8. Filament width (*W*) along the antennule. Tracks in wave-affected flow are shown in bars with black diagonal stripes (mean of all four wave-affected flow tracks in black bar), and tracks in unidirectional flow are shown in bars with gray diagonal stripes (mean of all three unidirectional flow tracks in gray bar). Values are means ± S.D. The number of flicks (*N*) for each track is shown in parentheses above the bar.

filaments in unidirectional flow, which is consistent with our comparison of filament widths as encountered by stomatopod antennules (Fig. 8).

The thinner filaments of lower odor concentration observed in the unidirectional flow condition are consistent with a more turbulent flow, as compared with the wave-affected case. Plumes in more turbulent flow experience higher strain rates as the eddies stretch odor-containing fluid into thinner, longer elements. The resulting increase in contact area between odored and non-odored fluid enhances mass transport by molecular diffusion as compared with plumes in less turbulent flows. Therefore, flows with higher levels of turbulence support thinner filaments with lower concentration peaks. This trend was observed by Moore et al. (1994). To compare levels of turbulence in the two flow situations, we collected velocity records in both flow conditions with a two-dimensional laser-Doppler anemometer (Dantec LDA operated in forward scatter mode with the same laser used for the PLIF data). Records with 200 000 velocity measurements were made at 63.5 Hz for the unidirectional flow, and with 120 000 points at 75.8 Hz for the wave-affected flow. We calculated u_* (the shear velocity; a measure of the turbulent fluctuations in velocity near the substratum), based on the slope of the logarithmic velocity profile, to be 0.25 cm s^{-1} for the unidirectional flow and 0.13 cm s^{-1} for the time-averaged velocity profile for the wave-affected flow. This suggests that, on average, the unidirectional flow is more turbulent than the wave-affected flow, supporting the observation of thinner filaments in the unidirectional flow. However, when we phase-averaged the wave-affected velocity signal at 10° increments, the values for u_* varied from 0 cm s^{-1} to 0.5 cm s^{-1}, with maximum values occurring at times when a high positive streamwise velocity was induced by wave motion. We are currently undertaking a detailed analysis of our hydrodynamic data, and we hope to address the issue of the turbulence characteristics of the wave-affected flow and the impact of the periodic changes in turbulence levels on dispersing odor plumes in a future manuscript.

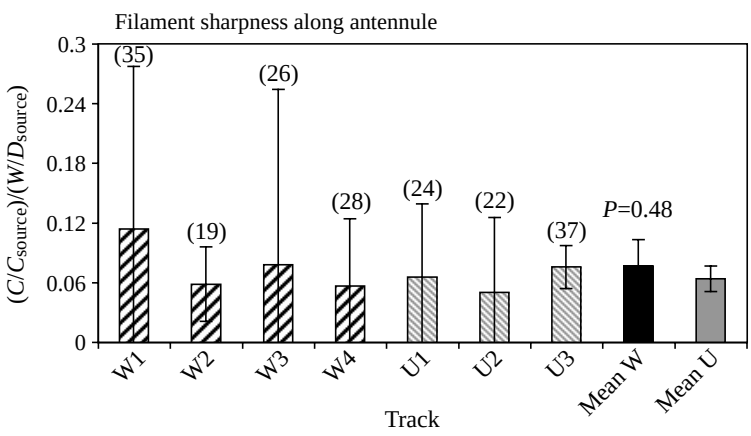

Fig. 9. Filament sharpness along the antennule. Filament sharpness is defined as the ratio of the maximum concentration, *C* (normalized by the source strength, C_{source}) to the spatial distance from the edge of the filament to the point of maximum concentration, *W* (normalized by the source diameter, D_{source}). Tracks in wave-affected flow are shown in bars with black diagonal stripes (mean of all four wave-affected flow tracks in black bar), and tracks in unidirectional flow are shown in bars with gray diagonal stripes (mean of all three unidirectional flow tracks in gray bar). Values are means ± S.D. The number of flicks (*N*) for each track is shown in parentheses above the bar.

General features of how animals encounter odor plumes

The way in which animals encounter odor plumes is a function of both the plume's physical structure and the animal's behavior. It has previously been assumed that animals in an odor plume are exposed to odor molecules nearly continuously. However, due to the sparseness of the plume, the fact that stomatopods sample odors with discrete flicks and the small size of their sensors, *H. ensiguera californica* can pass several seconds without encountering signal, even when they are in the middle of the odor plume and there are filaments nearby (Figs 2, 4). Despite the relatively low frequency of odor encounter, *H. ensiguera californica* located the odor source successfully in every trial (*N*=7) analyzed in this study. In addition, there is extreme variability in both time and space in the arrival of signal at the sensors. For instance, stomatopods can encounter a large, high-concentration filament during one flick and then encounter no signal on the next flick less than 0.2 s later (Fig. 4). Similarly, stomatopods can experience a large signal on one part of the antennule, while a neighboring segment of the antennule receives no odor. There is also great variability in the signal itself in terms of both peak odor concentration of the filaments and in the filament width.

Flow-dependent differences in odor plume sampling

A stomatopod flicking its antennules in wave-affected flow encounters filaments more frequently than animals in unidirectional flow (85% *versus* 63%). Odor filaments encountered by the antennules have a higher maximum odor concentration (Fig. 6A), a higher mean odor concentration (Fig. 6B) and appear wider (Fig. 8) in wave-affected flow than in unidirectional flow. As these differences in odor concentration along the antennules between wave-affected and unidirectional flow are minimized when plotted against available concentration, they appear to be due in large part to the differences in the physical characteristics of the plume between unidirectional and wave-affected flow rather than some aspect of the animals' behavior (Fig. 7).

In addition to differences in mean values, the variance of the filament concentration, filament width and filament sharpness is also greater in wave-affected flow than in unidirectional flow. Animals tracking plumes in wave-affected flow experience, on average, not only higher values of these parameters but also a wider variety of values than plume-tracking animals in unidirectional flow.

Our experiments have provided us with the instantaneous, fine-scale chemical signal encountered by mantis shrimp as they track odor plumes in wave-affected and unidirectional flow. The PLIF technique that we employed in this study permitted us to measure concentrations in an odor plume on the spatial and temporal scale at which they are encountered by the olfactory organs (antennules) of an animal while it is engaged in plume-tracking behavior. This information will enable us to correlate instantaneous plume-tracking behaviors with the fine-scale odor structure encountered by each of the animal's antennules.

We wish to thank R. L. Caldwell for sharing his stomatopod expertise, J. Crimaldi for his assistance with the PLIF, M. O'Donnell for helping with stomatopod collection and field velocity measurements, J. Fong for assistance with Y-maze experiments and protein determinations, and A. Albarico, S. Chang, J. Steinbuck and C. H. Yeung for digitization and other data analysis help. This project was funded by ONR Chemical Plume Tracing Program grant N00014-98-1-0775 to M. A. R. Koehl and ONR Chemical Plume Tracing Program grant N00014-98-1-0785 to J. R. Koseff.

References

Ache, B. W. (1982). Chemoreception and thermoreception. In *The Biology of Crustacea*, vol. 3 (ed. H. L. Atwood and D. C. Sandeman), pp. 369-393. New York: Academic Press.

Atema, J. (1985). Chemoreception in the sea: adaptations of chemoreceptors and behavior to aquatic stimulus conditions. *Soc. Exp. Biol. Symp.* **39**, 387-423.

Atema, J. (1988). Distribution of chemical stimuli. In *Sensory Biology of Aquatic Animals* (ed. J. Atema, R. R. Fay, A. N. Popper and W. Tavolga), pp. 29-56. New York: Springer-Verlag.

Atema, J. (1995). Chemical signals in the marine environment: dispersal, detection, and temporal signal analysis. In *Chemical Ecology: The Chemistry of Biotic Interaction* (ed. T. M. Eisner), pp. 147-159. Washington, DC: National Academy Press.

Atema, J., Moore, P. A., Madin, L. P. and Gerhardt, G. A. (1991). Subnore-1: electrochemical tracking of odor plumes at 900 m beneath the ocean surface. *Mar. Ecol. Prog. Ser.* **74**, 303-306.

Atema, J. and Voigt, R. (1995). Behavior and sensory biology. In *Biology of the Lobster* Homarus americanus (ed. J. R. Factor), pp. 313-348. San Diego: Academic Press.

Bossert, W. H. and Wilson, E. O. (1963). The analysis of olfactory communication among animals. *J. Theor. Biol.* **5**, 443-469.

Caldwell, R. L. (1979). Cavity occupation and defensive behaviour in the stomatopod *Gonodactylus festae*: evidence for chemically mediated individual recognition. *Anim. Behav.* **27**, 194-201.

Caldwell, R. L. (1982). Interspecific chemically mediated recognition in two competing stomatopods. *Mar. Behav. Physiol.* **8**, 189-197.

Caldwell, R. L. (1985). A test of individual recognition in the stomatopod *Gonodactylus festae*. *Anim. Behav.* **33**, 101-106.

Caldwell, R. L. (1987). Assessment strategies in stomatopods. *Bull. Mar. Sci.* **41**, 135-150.

Caldwell, R. L., Roderick, G. K. and Shuster, S. M. (1989). Studies of predation by *Gonodactylus bredini*. In *Biology of Stomatopods. Collana UZI, Selected Symposia and Monographs* (ed. E. A. Ferrero), pp. 117-131. Modena: Mucchi Editore.

Consi, T. R., Grasso, F., Mountain, D. and Atema, J. (1995). Exploration of turbulent odor plumes with an autonomous robot. *Biol. Bull.* **189**, 231-232.

Crimaldi, J. P. (1997). The effect of photobleaching and velocity fluctuations on single-point LIF measurements. *Exp. Fluids* **23**, 325-330.

Crimaldi, J. P. and Koseff, J. R. (2001). High-resolution measurements of the spatial and temporal scalar structure of a turbulent plume. *Exp. Fluids* **31**, 90-102.

Crimaldi, J. P., Wiley, M. B. and Koseff, J. R. (2002). The relationship between mean and instantaneous structure in turbulent passive scalar plumes. *J. Turbulence* **3**, 1-24.

Devine, D. V. and Atema, J. (1982). Function of chemoreceptor organs in spatial orientation of the lobster, *Homarus americanus*: differences and overlap. *Biol. Bull.* **163**, 144-153.

Dittmer, K., Grasso, F. and Atema, J. (1995). Effects of varying plume turbulence on temporal concentration signals available to orienting lobsters. *Biol. Bull.* **189**, 232-233.

Finelli, C. M., Pentcheff, N. D., Zimmer, R. K. and Wethey, D. S. (2000). Physical constraints on ecological processes: A field test of odor-mediated foraging. *Ecology* **81**, 784-797.

Fischer, H. B., List, E. J., Koh, R. C. Y., Imberger, J. and Brooks, N. H. (1979). *Mixing in Inland and Coastal Waters.* San Diego, CA: Academic Press.

Gleeson, R. A., Carr, W. E. S. and Trapido-Rosenthal, H. G. (1993). Morphological characteristics facilitating stimulus access and removal in the olfactory organ of the spiny lobster, *Panulirus argus*: insight from the design. *Chem. Senses* **18**, 67-75.

Gleeson, R. A., McDowell, L. M. and Aldrich, H. C. (1996). Structure of the aesthetasc (olfactory) sensilla of the blue crab, *Callinectes sapidus*: transformations as a function of salinity. *Cell Tissue Res.* **284**, 279-288.

Goldman, J. and Koehl, M. A. R. (2001). Fluid dynamic design of lobster olfactory organs: high-speed kinematic analysis of antennule flicking by *Panulirus argus*. *Chem. Senses* **26**, 385-398.

Gomez, G. and Atema, J. (1996a). Temporal resolution in olfaction: stimulus integration time of lobster chemoreceptor cells. *J. Exp. Biol.* **199**, 1771-1779.

Gomez, G. and Atema, J. (1996b). Temporal resolution in olfaction II: Time course of recovery from adaptation in lobster chemoreceptor cells. *J. Neurobiol.* **76**, 1340-1343.

Gomez, G., Voigt, R. and Atema, J. (1999). Temporal resolution in olfaction III: flicker fusion and concentration-dependent synchronization with stimulus pulse trains of antennular chemoreceptor cells in the American lobster. *J. Comp. Physiol. A* **185**, 427-436.

Grant, W. D. and Madsen, O. S. (1979). Combined wave and current interaction with a rough bottom. *J. Geophys. Res.* **84**, 1797-1808.

Hallberg, E., Johansson, K. U. I. and Wallén, R. (1997). Olfactory sensilla in crustaceans: morphology, sexual dimorphism, and distribution patterns. *Int. J. Insect Morphol. Embryol.* **26**, 173-180.

Kaissling, K. E. (1998a). Flux detectors versus concentration detectors: two types of chemoreceptors. *Chem. Senses* **23**, 99-111.

Kaissling, K. E. (1998b). Pheromone deactivation catalyzed by receptor molecules: a quantitative kinetic model. *Chem. Senses* **23**, 383-395.

Kemp, P. H. and Simons, R. R. (1982). The interaction between waves and a turbulent current: waves propagating with the current. *J. Fluid Mech.* **116**, 227-250.

Koehl, M. A. R. (1977). Effects of sea anemones on the flow forces they encounter. *J. Exp. Biol.* **69**, 87-105.

Koehl, M. A. R. (1982). The interaction of moving water and sessile organisms. *Sci. Am.* **247**, 124-134.

Koehl, M. A. R. (1984). How do benthic organisms withstand moving water? *Am. Zool.* **24**, 57-70.

Koehl, M. A. R. (1995). Fluid flow through hair-bearing appendages: feeding, smelling, and swimming at low and intermadiate Reynolds numbers. In *Biological Fluid Dynamics* (ed. C. P. Ellington and T. J. Pedley). *Soc. Exp. Biol. Symp.* **49**, 157-182. Cambridge: Company of Biologists Ltd.

Koehl, M. A. R. (1996). When does morphology matter? *Annu. Rev. Ecol. Syst.* **27**, 501-542.

Koehl, M. A. R., Koseff, J. R., Crimaldi, J. P., McCay, M. G., Cooper, T., Wiley, M. B. and Moore, P. A. (2001). Lobster sniffing: antennule design and hydrodynamic filtering of information in an odor plume. *Science* **294**, 1948-1951.

Louden, C., Best, B. and Koehl, M. A. R. (1994). When does motion relative to neighboring surfaces alter the flow through arrays of hairs? *J. Exp. Biol.* **193**, 233-254.

Mead, K. and Koehl, M. A. R. (2000). Particle image velocimetry measurements of fluid flow through a model array of stomatopod chemosensory sensilla. *J. Exp. Biol.* **203**, 3795-3808.

Mead, K., Koehl, M. A. R. and O'Donnell, M. J. (1999). Stomatopod sniffing: the scaling of chemosensory sensilla and flicking behavior with body size. *J. Exp. Mar. Biol. Ecol.* **241**, 235-261.

Mead, K. and Weatherby, T. (2002). The morphology of stomatopod chemosensory sensilla facilitates fluid sampling. *Inv. Biol.* **121**, 148-157.

Moore, P. A. (1994). A model of the role of adaptation and disadaptation in olfactory receptor neurons: Implications for the coding of temporal and intensity patterns in odor signals. *Chem. Senses* **19**, 71-86.

Moore, P. A. and Atema, J. (1988). A model of a temporal filter in chemoreception to extract directional information from a turbulent odor plume. *Biol. Bull.* **174**, 355-363.

Moore, P. A. and Atema, J. (1991). Spatial information in the three-dimensional fine-structure of an aquatic odor plume. *Biol. Bull.* **181**, 408-418.

Moore, P. A., Atema, J. and Gerhardt, G. A. (1991). Fluid dynamics and microscale chemical movement in the chemosensory appendages of the lobster, *Homarus americanus*. *Chem. Senses* **16**, 663-674.

Moore, P. A., Grills, J. L. and Schneider, R. W. S. (2000). Habitat-specific signal structure for olfaction: an example from artificial streams. *J. Chem. Ecol.* **26**, 565-584.

Moore, P. A., Weissburg, M. J., Parrish, J. M., Zimmer-Faust, R. K. and Gerhardt, G. A. (1994). The spatial distribution of odors in simulated benthic boundary layer flows. *J. Chem. Ecol.* **20**, 255-279.

Murlis, J. and Jones, C. D. (1981). Fine-scale structure of odour plumes in relation to insect orientation to distant pheromone and other attractant sources. *Physiol. Entomol.* **6**, 71-86.

Pidgeon, E. J. (1999). An experimental investigation of breaking wave induced turbulence. *PhD dissertation*, Stanford University.

Reeder, P. B. and Ache, B. W. (1980). Chemotaxis in the Florida spiny lobster *Panulirus argus*. *Anim. Behav.* **28**, 831-839.

Rospars, J.-P., Křivan, V. and Lánsky, P. (2000). Perireceptor and receptor events in olfaction. Comparison of concentration and flux detectors: a modeling study. *Chem. Senses* **25**, 293-311.

Schmidt-Nielsen, K. (1990). *Animal Physiology: Adaptation and Environment*, 4th edn. Cambridge: Cambridge University Press.

Schmitt, B. C. and Ache, B. W. (1979). Olfaction: responses of a decapod crustacean are enhanced by flicking. *Science* **205**, 204-206.

Snow, P. J. (1973). Ultrastructure of the aesthetasc hairs of the littoral decapod, *Paragrapsus gaimardii*. *Z. Zellforsch.* **138**, 489-502.

Stacey, M. T., Mead, K. S. and Koehl, M. A. R. (2002). Molecular capture by olfactory antennules: mantis shrimp. *J. Math. Biol.* **44**, 1-30.

Steullet, P. and Derby, C. D. (1997). Coding of blend ratios of binary mixtures by olfactory neurons in the Florida spiny lobster, *Panulirus argus*. *J. Comp. Physiol. A* **180**, 123-135.

Webster, D. R., Rahman, S. and Dasi, L. P. (2001). On the usefulness of bilateral comparison to tracking turbulent chemical odor plumes *Limnol. Oceanogr.* **46**, 1048-1053.

Webster, D. R. and Weissburg, M. J. (2001). Chemosensory guidance cues in a turbulent chemical odor plume. *Limnol. Oceanog.* **46**, 1034-1047.

Weissburg, M. J. (2000). The fluid dynamical context of chemosensory behavior. *Biol. Bull.* **198**, 188-202.

Weissburg, M. J. and Zimmer-Faust, R. K. (1993). Life and death in moving fluids: hydrodynamic effects on chemosensory-mediated predation. *Ecology* **74**, 1428-1443.

Weissburg, M. J. and Zimmer-Faust, R. K. (1994). Odor plumes and how blue crabs use them in finding prey. *J. Exp. Biol.* **197**, 349-375.

Zettler, E. and Atema, J. (1999). Chemoreceptor cells as concentration slope detectors: preliminary evidence from the lobster nose. *Biol. Bull.* **197**, 252-253.

Zimmer-Faust, R. K. (1989). The relationship between chemoreception and foraging behavior in crustaceans. *Limnol. Oceanogr.* **34**, 1364-1374.

Zimmer-Faust, R. K., Finelli, C. M., Pentcheff, N. D. and Wethey, D. S. (1995). Odor plumes and animal navigation in turbulent water flow: a field study. *Biol. Bull.* **188**, 111-116.

Zimmer-Faust, R. K., Gleeson, R. A. and Carr, W. E. (1988a). The behavioral response of spiny lobsters to ATP: evidence for mediation by P-2-like chemosensory receptors. *Biol. Bull.* **175**, 167-174.

Zimmer-Faust, R. K., Stanfill, J. M. and Collard, S. B., III (1988b). A fast multichannel fluorometer for investigating aquatic chemoreception and odor trails. *Limnol. Oceanogr.* **33**, 1586-1595.